P7.7 SENSITIVITY OF TROPICAL SUBANNUAL VARIABILITY TO MODEL MIXED-LAYER DEPTH

I. G. Watterson
CSIRO Atmospheric Research

1. INTRODUCTION

The role of air-sea interaction in inducing tropical variability on subannual timescales remains unclear. It is well recognised, however, that general circulation models (GCMs) with noninteracting specified sea surface temperatures (SSTs) are deficient in their simulation of the eastward propagating 30–60 d variability of the Madden-Julian Oscillation (MJO). In observations, Kawamura (1991) detected higher SSTs to the east of low-level convergence associated with the MJO, and noted that this could enhance propagation. Flatau et al. (1997) simulated such an enhancement using a simple parameterization of interaction. The present study was motivated by the analysis of anomalies in the Australasian monsoon in the CSIRO Mark 2 GCM by Watterson (2001). Slow, eastward propagation occurred in the coupled atmosphere–ocean model (C) but not in the specified SST model (S). An extensive analysis of monthly mean data from December–February indicates that the anomalies are related to MJO-like tropical patterns (c.f. Hendon and Liebmann, 1990) and that higher SSTs appear to lead them, both in the C case, and in a run (M50) with a model with a simple 50-m deep mixed-layer ocean (the depth being close to that of the tropical mixed layer of the coupled model). Since the local periods in the variation are evidently in the 100–200 d range, longer than the MJO, we consider whether an enhancement of the interaction, achieved by reducing the mixed-layer depth, can result in more realistic periods.

2. EOF ANALYSIS FOR JANUARY

We focus here on an analysis of 20–365 d band-pass filtered daily data available over 100 years of C, M50, and S (the band being broader than the usual 20–100 d of MJO studies). As in Watterson (2001), we determine empirical orthogonal functions (EOFs) of the tropical σ = 0.8 wind vectors from all January days of C. The first two EOFs each have a broad pattern including a convergent core, resembling phases of the MJO. Their dominant zonal wind u component is largest within the mean westerly belt, as depicted in Fig. 1. EOF2 is related to the monsoon anomaly, with a westerly peak over the Timor Sea and a v component onto northeastern Australia.

The time series (or principal component, with standard deviation SD = 1) associated with EOF2 represents an amplitude factor or index for each January day. Regression with the (lag 0) winds reproduces the EOF, while using lagged winds allows a depiction of its evolution and persistence. Slow eastward propagation for C is clear from the lag 14 d result in Fig. 2b (and other positive and negative lag results, not shown), consistent with the previous monthly result. Projecting EOF2 on the daily (filtered) wind data of S produces an index for that run, whose regressions with u depict weaker persistence, and, if anything, slow westward propagation (Fig. 2a). With the M50 result again similar to C, 50-year simulations with the mixed-layer depth reduced to 20 m or 10 m between 19°S and 19°N were performed, and denoted M20 and M10. The prescribed layer heating fields were recalculated, in each case, so that the observed SST annual cycle is closely maintained, as are the climatological winds. The persistence and propagation speed are, indeed, further enhanced as the depth is decreased (Fig. 2c).

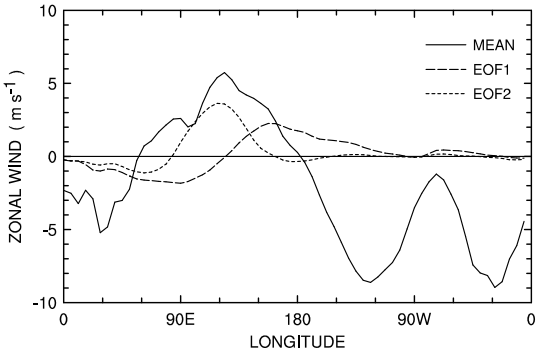

Figure 1: Zonal wind at σ = 0.8 in January from run C averaged over 13°S to 3°N. Shown are the climatatological mean, and the u component of EOF1 and EOF2 from 20–365 d filtered daily wind vectors in tropics.

3. AIR-SEA INTERACTION

The SST anomalies related to the EOF2 index in M10 are shown in Fig. 3. Temperatures drop near 120°E as the wind surge augments the westerly mean flow (around lag 0), leading to enhanced evaporation. To the east SSTs initially rise due to an easterly anomaly and enhanced solar radiation. The mechanism is similar in C, but the changes are slower, due to the deeper mixed layer. The SST anomalies are a little larger in M10 but appear similar to those observed. The negative anomalies forming to the east of the low-level divergence tend to induce divergence over them, resulting in an eastward tendency across the mean westerly belt. This counters a weak tendency for westward propagation that follows from wind-evaporative feedback, except in S.

A similar analysis of subannual variability in the central months of other seasons shows that air-sea interaction

Corresponding author address: Ian G. Watterson, CSIRO Atmospheric Research, Private Bag 1, Aspendale 3195, Australia; e-mail igw@dar.csiro.au

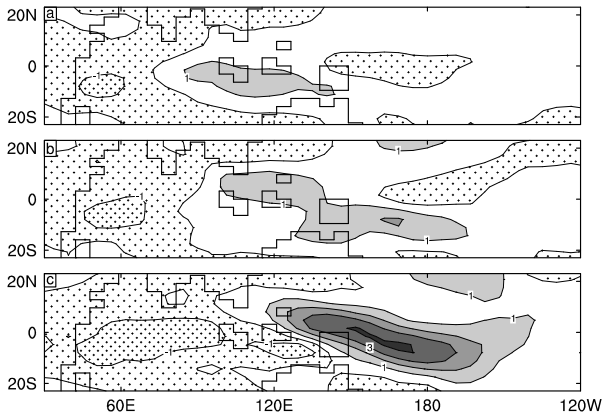

Figure 2: Regression field (the regression coefficient $\times$ 1 index SD) of σ = 0.8 u (m s^{-1}) lagged 14 d with the band-passed January EOF2 index: (a) run S, (b) run C, and (c) run M10.

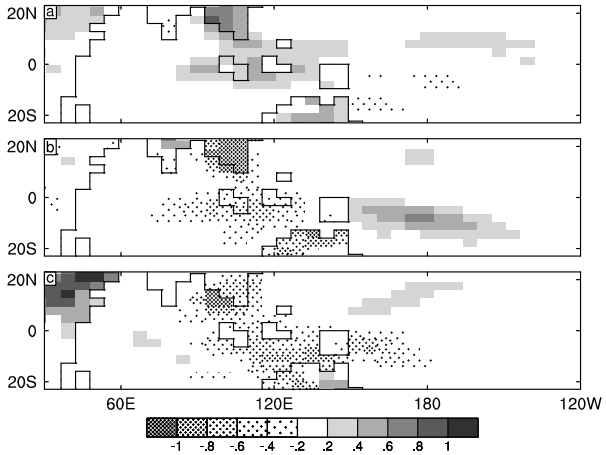

Figure 3: Regression surface temperature (K) with the band-passed January EOF2 index in run M10: (a) lag $-$14 d, (b) lag 0, (c) lag 14 d.

generally enhances the amplitude and persistence of the MJO-like EOF1 and 2 patterns. Their eastward propagation is enhanced over the westerly wind belt, and more so as the mixed-layer depth decreases. However, as this belt is shorter in April and October, and shifted northward in July, the enhancement is not as strong as in January.

4. **WAVE-1 SPECTRA**

The MJO features a large-scale return flow circulation in the upper troposphere coherent with the low-level convergence, and this is seen for the simulated EOF patterns also. A standard MJO signal is the enhanced power over 30–60 d in the spectrum of the eastward propagating component of the zonal wavenumber one, equatorial, upper-level zonal winds. In the S model spectrum (Fig. 4) there is a little more eastward component, than westward, across the whole subannual range, with only a weak peak at 30 d. Consistent with the slow eastward propagation of MJO-like circulations seen in some seasons, the M50

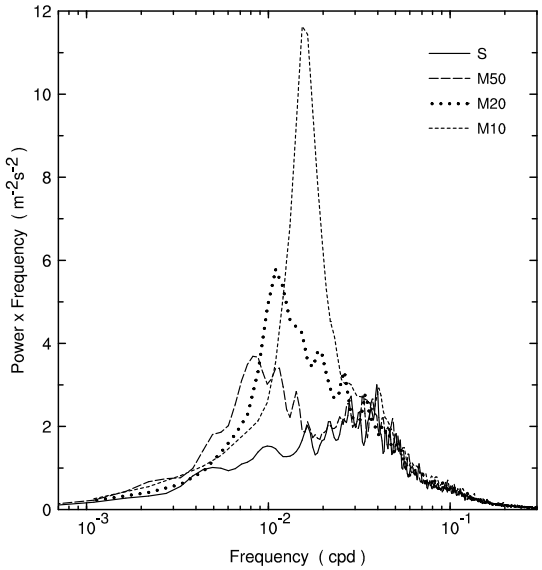

Figure 4: Spectrum of eastward propagating component of wave-1 u at σ = 0.2 over 10°S–10°N, from four runs.

eastward spectrum is enhanced over 80–200 d (by a little more at the shorter periods than for C). As the mixed-layer depth is decreased the peak increases dramatically in amplitude and frequency. The M10 peak is twice that observed, and its period, 65 d, is near the MJO band.

5. **CONCLUSIONS**

The analysis indicates that air-sea interaction can have a dramatic effect on simulated eastward propagating tropical variability at subannual periods. Propagation is particularly enhanced over the convective, low-level westerly belt bridging the Indian and Pacific Oceans in the CSIRO GCM. Given the apparent realism of this feature, the results suggest that interaction may be crucial to the MJO, if it is as vigorous as it is in the present shallow mixed-layer model.

REFERENCES

Flatau, M., P. J. Flatau, P. Phoebus, and P. P. Niiler, 1997: The feedback between equatorial convection and local radiative and evaporative processes: the implications for intraseasonal oscillation. *J. Atmos. Sci.*, **54**, 2373–2386.

Hendon, H. H., and B. Liebmann, 1990: The intraseasonal (30–50-day) oscillation of the Australian summer monsoon. *J. Atmos. Sci.*, **47**, 2909–2923.

Kawamura, R., 1991: Air-sea coupled modes on intraseasonal and interannual time scales over the tropical western Pacific. *J. Geophys. Res.*, **96**, 3165–3172.

Watterson, I. G., 2001: Wind-induced rainfall and surface temperature anomalies in the Australian region. *J. Climate*, **14**. in press.